ISSN 0016-7029, Geochemistry International, 2006, Vol. 44, No. 7, pp. 636–655. © Pleiades Publishing, Inc., 2006.
Original Russian Text © I.T. Rass, S.S. Abramov, V.A. Utenkov, V.M. Kozlovskii, D.I. Korpechkov, 2006, published in Geokhimiya, 2006, No. 7, pp. 692–711.

Role of Fluid in the Genesis of Carbonatites and Alkaline Rocks: Geochemical Evidence

I. T. Rass[a], S. S. Abramov[a], V. A. Utenkov[b], V. M. Kozlovskii[a], and D. I. Korpechkov[a]

[a]*Institute of Geology of Ore Deposits, Petrography, Mineralogy, and Geochemistry, Russian Academy of Sciences, Staromonetnyi per. 35, Moscow, 119017 Russia*

e-mail: rass@igem.ru

[b]*Moscow State Geological Prospecting University, ul. Miklukho-Maklaya 23, Moscow, 117997 Russia*

Received October 27, 2004

Abstract—In most alkaline–ultrabasic–carbonatite ring complexes, the distribution of trace elements in the successive derivatives of mantle magmas is usually controlled by the Rayleigh equation of fractional crystallization in accordance with their partition coefficients, whereas, that of late derivatives, nepheline syenites and carbonatites, is usually consistent with trends characteristic of silicate–carbonate liquid immiscibility. In contrast to the carbonatites of ring complexes, carbonatites from deep-seated linear zones have no genetic relation with alkaline–ultrabasic magmatism, and the associated alkaline rocks are represented only by the nepheline syenite eutectic association. The geochemical study of magmatic rocks from the Vishnevye Gory nepheline syenite–carbonatite complex (Urals), which is assigned to the association of deep-seated linear zones, showed that neither differentiation of a parental melt nor liquid immiscibility could produce the observed trace element distribution (Sr, Rb, REE, and Nb) in miaskites and carbonatites. Judging from the available fragmentary experimental data, the distribution patterns can be regarded as possible indicators of element fractionation between alkaline carbonate fluid and alkaline melt. Such trace element distribution is presumably controlled by a fluid–melt interaction; it was also observed in carbonatites and alkaline rocks of some ring complexes, and its scarcity can be explained by the lower density of aqueous fluid released from magma at shallower depths.

DOI: 10.1134/S0016702906070020

INTRODUCTION

There are significant differences in the character of trace element fractionation related to the differentiation of alkaline ultrabasic melts, immiscibility of carbonatite and alkaline melts, and the interaction between a melt (carbonate or silicate) and a fluid. In most alkaline–ultrabasic–carbonatite ring complexes, the distribution of trace elements in the successive derivatives of mantle magmas is usually described by Rayleigh fractional crystallization in accordance with their partition coefficients; whereas the compositions of late derivatives, nepheline syenites, and carbonatites are usually consistent with the characteristic features of silicate–carbonate liquid immiscibility. The resulting chondrite-normalized distribution patterns of, for example, REE in the alkaline rocks derived from these magmas [1] and carbonatites [2] are smooth functions of their ionic radius and atomic number.

However, in many cases the distribution of trace elements cannot be explained by either fractional crystallization or liquid immiscibility. In particular, immiscibility between two melts was probably not the main control of the trace element distribution observed in the silicate rocks and natrocarbonatites of Oldoinyo Lengai [3]. There are cases when REE distribution both in silicate rocks and carbonatites cannot be explained by fractional crystallization. For example, according to [4], the REE distribution patterns in successive derivatives [alkaline picrite–nephelinite (Hanang Volcano), melanephelinite–nephelinite (Moroto Volcano), melanephelinite–phonolite (Eldoret Volcano)] display a negative Eu anomaly increasing toward the later derivatives; the same is observed in the nephelinite–phonolite–carbonatite series (Oldoinyo Lengai, eruption of 1966?); whereas REE distribution in the ijolite–melteigite of the Napak Massif, Uganda, exhibits a tetrad effect. According to other data, the silicate lavas of Oldoinyo Lengai (eruption of 1983?) show a weak Eu anomaly [5]. The REE distribution patterns in the phonolite and carbonatite of the Kaiserstuhl Massif show negative and positive Eu anomalies, respectively (according to [6]). A negative Eu anomaly was reported for some carbonatites from the East African Rift [4], Guli Massif in NW Siberia [7], syenites of Magnet Cove [8], and some melilitites from Germany [9]; a positive Eu anomaly was observed in the REE patterns of ijolites and monticellite–diopside carbonatites of the Oka Massif, Canada [10].

The presence of a negative Eu anomaly in the REE distribution pattern of alkaline–ultrabasic rocks and carbonatites of ring complexes cannot be explained by plagioclase fractionation, because plagioclase is lacking in them.

In addition to fractional crystallization and liquid immiscibility, which usually control the distribution of trace elements in the carbonatites and alkaline rocks of ring complexes, fluid–rock or fluid–melt (silicate or carbonate) interactions may be of great importance. It was experimentally shown that the efficiency of REE fractionation caused by the interaction of aqueous chloride fluid with an ultra-alkaline melt is comparable or even stronger than that related to crystallization differentiation [11].

The development of giant fenite halos around alkaline–ultrabasic–carbonatite ring massifs provides compelling evidence for the existence of alkaline fluids genetically related to mantle derivatives, both silicate rocks and carbonatites [12, 13]. According to experimental data [14], alkaline fluids can be highly concentrated. In the past decade, orthomagmatic fluids bearing Na, K, Ca, Cl^-, HCO_3^-, CO_3^{2-}, and other components were found in many magmatic inclusions in the minerals of both carbonatites and alkaline ultrabasic rocks [15, 16].

Experimental studies on the partitioning of trace elements between melt and fluid are still scarce and fragmentary, i.e., restricted to narrow ranges of either physicochemical parameters or compositions of melts and/or fluids. In order to better understand the character of trace element partitioning, we performed a study of nepheline syenites and carbonatites from the Vishnevye Gory massif in the Urals. Their formation is a natural experiment in which the differentiation of primary alkaline ultrabasic magmas is excluded, because the carbonatites of deep-seated linear zones (including the Vishnevye Gory nepheline syenite–carbonatite massif), unlike the carbonatites of ring complexes, have no genetic relation with alkaline ultrabasic magmatism [17], and the only accompanying alkaline rocks are the nepheline syenites (miaskites) of the eutectic association.

The Vishnevye Gory alkaline complex (55°59′ N; 60°34′ E) is situated in the eastern slope of the Urals [18–20] among the Early Proterozoic (~2 Ga) plagiogneisses and amphibolites of the Vishnevye Gory Formation and confined to an anticlinal structure with an SW-plunging hinge. Owing to this, a major portion of the complex, from the near-root zone at the Potaniny Mountains to the apical zone at the Vishnevye Mountains, is exposed and accessible for study (Fig. 1). The erosion depth is 7–10 km. The carbonatites belong to the high-temperature (>530°C) calcite–feldspar facies [21] of the association of linear zones. Their isotopic and trace-element characteristics suggest mantle origin [22, 23] for these rocks.

In the root zone of the massif (Potaniny Mountains, vermiculite quarry), we studied the geochemistry of successive zones of plagiogneiss fenitization, alkaline igneous rocks, and miaskites: plagiogneiss–fenitized plagiogneiss–pyroxene fenite–biotite-feldspar rock–nepheline migmatite–antiperthite miaskite. Another target for the geochemical study were the successive metasomatic zones developed after amphibolites: amphibolite–amphibole-plagioclase-biotite rock–plagioclase-biotite-calcite rock–biotite-calcite rock with plagioclase–melanocratic biotite carbonatite. The width of the metasomatic zones in the root part of the complex varies in the plan view from 40 to 400 m [20].

In the apical zone of the massif (Vishnevye Mountains, Dolgaya and Mokhnataya mounts), two-feldspar miaskites, including calcite-bearing varieties (up to 10–12% calcite in equilibrium with nepheline and K feldspar), carbonatites and metasomatic rocks were studied. The latter compose successive zones of miaskite-related fenitization of the plagiogneisses of the same formation (Vishnevye Gory): plagiogneiss–biotite fenite–amphibole fenite–pyroxene fenite–miaskite. The chemical compositions of the rocks are shown in Tables 1 and 2.

GEOCHEMISTRY OF IGNEOUS ROCKS

The compositions of the miaskites of the Vishnevye Gory Complex vary within a narrow range, with a minor increase in alkalis and Ca content from the root to the apical zones and further to the calcite-bearing miaskites (Fig. 2). The compositions of carbonatites follow the curve of liquid immiscibility experimentally determined at 2–5 kbar and 900°C [24]. The points of carbonatite–syenite from the Malyi Kovdor ring massif, Kola Peninsula, fall close to them [25]. The average partition coefficients of Ti, Mn, and trace elements between the carbonatites and nepheline syenites (miaskites) of the Vishnevye Gory Complex (Table 3) are significantly different from those calculated for the ring complexes (for example, East African Rift), as well as from the values experimentally determined within a wide temperature and pressure range typical of liquid immiscibility. The geochemistry of the antiperthite miaskites and corresponding carbonatites of the root zone, as well as the two-feldspar miaskites (including calcite-bearing ones) and corresponding carbonatites of the apical zone rules out a liquid immiscibility origin.

The contents of a number of trace elements in the miaskites and carbonatites of the root and apical zones of the complex are shown in binary logarithmic plots (Fig. 3). It should be noted that both carbonatites and miaskites of the Vishnevye Mountains have notably higher contents of Mn (up to 2.4 and 0.33% MnO, respectively), Rb (up to 723 and 230 ppm), and Nb (up to 1450 and 485 ppm) than the carbonatites and miaskites of the Potaniny Mountains (<0.58 and 0.15% MnO, <72 and 33 ppm Rb, <643 and 359 ppm Nb, respectively). By contrast, the rocks of the Potaniny Mountains show higher contents of Ba and P_2O_5 (up to 1836 ppm Ba and 1.5% P_2O_5 in the carbonatites and 4375 ppm Ba and 0.92% P_2O_5 in the miaskites) compared to the carbonatites (up to 755 ppm Ba and 0.42%

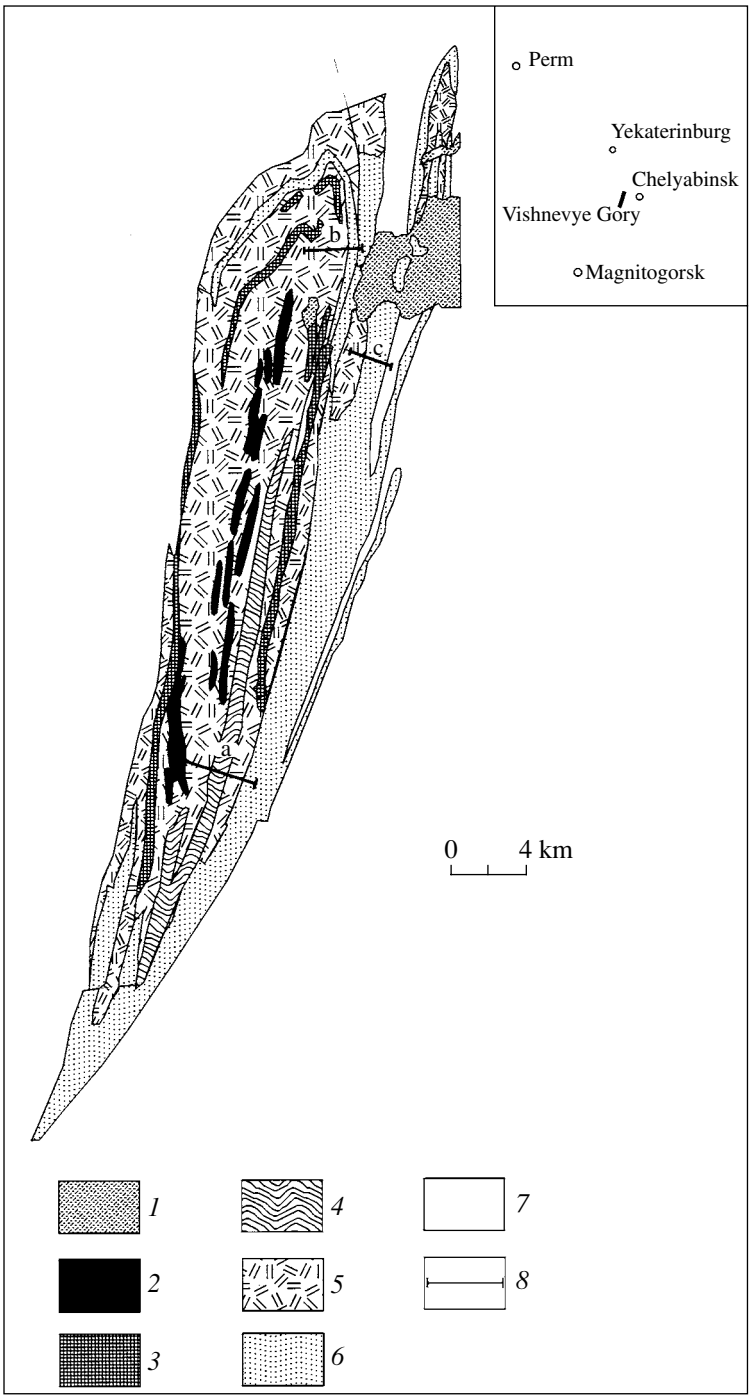

Fig. 1. Geological sketch map of the Vishnevye Gory Massif [18, 19]. (*1*) Sediments; (*2*) carbonatite; (*3*) albitite; (*4*) pyroxene fenite, biotite–feldspar rock, and nepheline migmatite; (*5*) nepheline syenite; (*6*) fenitized plagiogneiss and amphibole fenite; (*7*) plagiogneiss, amphibolite, and schist; (*8*) profiles: (a) in the root zone of the complex (Potaniny Mountains, vermiculite quarry), (b, c) in the apical zone of the complex (Vishnevye Mountains, Vishnevogorsk area, Dolgaya and Mokhnataya mounts).

P_2O_5) and miaskites (1081 ppm Ba and 0.19% P_2O_5) of the Vishnevye Mountains.

The carbonatites of the root and apical zones have the highest REE abundances among the rocks of the complex and have a somewhat different REE distribution patterns. The carbonatites of the root zone have a smooth almost linear pattern with notable LREE enrichment, whereas the carbonatites of the apical zone have a more fractionated LREE pattern (La/Gd = 22–27 compared with 8–13 in the root zone) and an almost horizontal HREE pattern (Gd/Yb = 1.7–2.0 compared with 4–6 in the root zone) (Fig. 4a).

Table 1. Chemical composition of rocks from the root zone (oxides in wt %, elements in ppm)

Component	Plagiogneiss		Fenitized plagiogneiss			Fenite						Biotite–feldspar rock	
	Sample no.												
	410	609	607	603	606B	409	407	418	566-19	601	567	400-2	566
SiO_2	76.54	72.94	67.89	64.75	62.67	64.39	64.24	64.69	64.66	60.65	63.26	58.83	53.90
TiO_2	0.12	0.25	0.15	0.25	0.33	0.45	0.49	0.96	0.88	1.03	0.52	0.30	2.00
Al_2O_3	11.27	12.64	16.92	17.33	20.18	17.74	17.80	13.17	13.04	12.91	16.99	21.91	17.30
Fe_2O_3	2.76	3.13	0.96	2.51	1.88	2.25	2.17	7.11	7.30	7.32	2.99	2.22	6.48
MnO	0.018	0.027	0.02	0.055	0.036	0.060	0.061	0.161	0.179	0.308	0.055	0.032	0.15
MgO	0.02	0.15	0.05	0.09	0.31	0.20	0.24	1.40	1.13	1.27	0.53	0.47	1.85
CaO	0.35	0.97	0.36	0.53	0.70	1.08	1.12	3.50	3.76	3.68	0.99	1.02	7.11
Na_2O	2.97	2.73	4.28	5.25	6.31	4.56	4.40	3.64	3.57	5.44	5.55	7.44	4.32
K_2O	4.80	5.67	6.69	6.37	3.62	6.64	7.20	3.55	3.42	3.53	3.97	4.07	2.87
P_2O_5	0.012	0.037	0.030	0.08	0.084	0.059	0.126	0.265	0.338	0.457	0.005	0.054	0.482
Total	98.89	98.65	98.10	97.64	96.80	97.53	98.27	98.55	98.38	96.88	96.16	96.68	97.50
Cr	<10	<10	<10	<10	<10	<10	<10	<10	<10	13	<10	<10	<10
Ni	<10	<10	<10	<10	<10	<10	<10	15	11	12	<10	<10	<10
Co	<10	<10	<10	<10	<10	<10	<10	12	13	<10	<10	<10	<10
V	25	<20	<20	35	31	<20	<20	83	72	153	56	66	92
Zr	153	276	84	43	243	178	210	422	512	479	125	1423	160
Nb	<10	18	62	55	34	108	72	31	44	198	31	13	145
Sc	<10	<10	<10	14	<10	<10	<10	21	11	21	<10	<10	12
Y	<10	56	12	15	<10	23	18	64	68	60	<10	<10	46
Sr	34	118	778	389	2080	211	507	868	1567	600	3399	1641	3137
Ba	143	573	4971	3099	3386	358	1084	1823	1427	1621	6914	1466	5177
Rb	104	349	131	94	56	130	120	148	132	92	42	57	47
La	–	92.1	–	–	–	47.5	–	–	–	150	–	120	95.8
Ce	–	171	–	–	–	117	–	–	–	360	–	235	247
Pr	–	17.8	–	–	–	12.1	–	–	–	40	–	27.9	31.8
Nd	–	55.8	–	–	–	39.2	–	–	–	143	–	104	125
Sm	–	8.62	–	–	–	5.48	–	–	–	21.4	–	18.4	21.8
Eu	–	1.7	–	–	–	1.42	–	–	–	4.67	–	4.73	6.84
Gd	–	6.34	–	–	–	3.51	–	–	–	14.8	–	12.9	15
Tb	–	0.88	–	–	–	0.59	–	–	–	2.06	–	1.74	1.97
Dy	–	5.54	–	–	–	3.57	–	–	–	10.8	–	8.74	10.4
Ho	–	1.06	–	–	–	0.7	–	–	–	2.12	–	1.5	1.84
Er	–	3.09	–	–	–	1.93	–	–	–	5.62	–	3.54	3.97
Tm	–	0.43	–	–	–	0.3	–	–	–	0.81	–	0.44	0.54
Yb	–	2.7	–	–	–	1.65	–	–	–	5.07	–	2.62	2.41
Lu	–	0.39	–	–	–	0.28	–	–	–	0.86	–	0.35	0.34
REE	–	367.45	–	–	–	235.23	–	–	–	761.21	–	541.86	564.71

Table 1. (Contd.)

Component	Biotite–feldspar rock				Migmatite					Antiperthite miaskite			
	Sample no.												
	608	406	408	606A	318	318-1	318-2	3423-140	604	3423-90a	3423-90b	306	320
SiO_2	55.01	59.02	59.61	57.8	51.34	63.39	48.65	54.23	58.95	57.38	61.43	59.29	54.37
TiO_2	1.48	1.10	1.38	0.85	0.55	0.18	0.67	0.78	0.46	0.52	0.30	0.59	0.38
Al_2O_3	15.72	12.57	12.23	22.35	26.31	20.86	26.82	21.45	20.95	21.57	20.96	19.47	21.98
Fe_2O_3	8.67	8.04	8.75	4.41	3.90	2.36	5.03	3.69	2.99	3.22	2.11	3.48	3.16
MnO	0.170	0.228	0.27	0.086	0.066	0.038	0.097	0.082	0.053	0.029	0.014	0.073	0.056
MgO	1.22	0.91	0.89	1.08	1.43	0.38	1.79	0.66	0.55	0.68	0.42	1.19	0.85
CaO	5.41	4.24	5.11	0.67	2.53	3.86	2.68	2.27	1.02	1.36	0.35	3.43	4.48
Na_2O	3.77	4.64	4.49	5.90	6.87	7.08	7.16	6.90	7.41	7.09	6.64	5.56	6.87
K_2O	3.49	4.32	4.22	4.15	3.65	0.75	4.59	5.19	4.01	4.44	4.50	3.66	1.93
P_2O_5	0.519	0.407	0.520	0.024	0.068	0.140	0.107	0.105	0.14	0.303	0.030	0.265	0.249
Total	95.75	95.82	97.83	97.99	96.76	97.09	97.65	95.41	97.07	96.66	96.84	97.04	94.37
Cr	<10	<10	<10	10	<10	<10	<10	<10	<10	<10	<10	<10	10
Ni	16	17	17	11	11	<10	<10	10	10	10	<10	<10	11
Co	12	<10	13	<10	<10	<10	<10	<10	<10	<10	<10	<10	<10
V	98	76	88	63	108	98	137	65	39	70	39	54	76
Zr	571	510	537	3415	1484	109	1399	536	369	1670	117	62	448
Nb	71	58	98	52	17	<10	32	105	31	172	65	17	<10
Sc	19	18	24	<10	<10	<10	<10	<10	<10	<10	<10	<10	<10
Y	114	65	70	13	10	<10	18	16	<10	14	<10	<10	<10
Sr	465	913	1023	2292	2655	4158	1864	1767	1353	779	714	2598	2856
Ba	1594	1729	1782	3278	2663	2732	2499	3657	2938	3607	4232	4375	2854
Rb	92	109	104	85	57	22	71	97	67	82	67	54	33
La	172	180	–	–	16.4	24.7	27.3	26.4	n.d.	64.6	19.4	28.7	31.5
Ce	413	399	–	–	26.9	38.5	45.5	48.8	″	119	30.8	58.1	53.4
Pr	48.1	41.6	–	–	2.66	4	4.49	5.28	″	13.1	2.92	6.89	5.44
Nd	186	148	–	–	8.4	13.6	14.5	17.4	″	43.1	8.6	25	19.4
Sm	33.8	21.4	–	–	1.63	2.1	2.12	2.84	″	5.23	1.11	4.12	3.06
Eu	6.07	4.51	–	–	<0.07	<0.07	<0.07	<0.07	″	0.17	<0.07	<0.07	<0.07
Gd	24.2	15	–	–	1.34	1.48	1.54	1.74	″	2.51	0.65	3.22	2.12
Tb	3.59	2.07	–	–	0.14	0.17	0.21	0.25	″	0.31	0.07	0.4	0.27
Dy	21	11.8	–	–	0.83	0.97	1.15	1.39	″	1.51	0.26	1.85	1.6
Ho	4.23	2.3	–	–	0.18	0.19	0.24	0.21	″	0.28	0.07	0.36	0.31
Er	11.7	6.19	–	–	0.5	0.46	0.63	0.73	″	0.69	0.15	0.95	0.86
Tm	1.59	0.86	–	–	0.07	0.07	0.08	0.1	″	0.09	0.02	0.12	0.12
Yb	10.3	5.35	–	–	0.5	0.47	0.72	0.52	″	0.53	0.19	0.76	0.64
Lu	1.54	0.89	–	–	0.08	0.08	0.1	0.09	″	0.07	0.03	0.08	0.12
REE	937.12	838.97	–	–	59.64	86.8	98.59	105.76	″	251.19	64.28	130.56	118.85

Table 1. (Contd.)

Component	Antiperthite miaskite				Amphibolite			Amphibole–plagioclase–biotite rock			Plagioclase–biotite rock with calcite		
	Sample no.												
	316Å	602A	602B	419	3316-329	3316-304	610	569	411	3411-531	402	311	313
SiO_2	57.50	57.07	58.52	52.86	57.05	51.5	49.21	48.24	54.96	50.79	39.53	44.31	38.52
TiO_2	0.61	1.18	0.39	0.46	0.43	1.29	1.17	1.79	1.28	1.06	4.30	3.74	4.15
Al_2O_3	21.63	18.59	20.84	19.39	13.93	13.22	11.28	15.34	14.25	15.21	10.90	6.89	11.77
Fe_2O_3	4.74	4.53	3.12	3.19	8.28	11.48	15.67	9.83	8.89	10.21	16.00	13.24	17.00
MnO	0.077	0.154	0.083	0.076	0.141	0.157	0.224	0.22	0.203	0.182	0.300	0.289	0.320
MgO	0.70	0.93	0.32	0.70	3.66	4.6	7.22	4.86	3.31	8.38	13.49	8.88	6.72
CaO	1.62	2.28	0.71	5.41	6.25	6.84	9.79	7.00	6.54	9.63	6.83	15.67	13.65
Na_2O	6.57	6.04	7.14	5.88	2.91	2.54	1.69	3.72	4.63	3.85	1.16	2.22	2.77
K_2O	4.50	4.72	5.07	4.84	1.28	2.35	0.68	5.19	2.18	2.09	6.13	2.14	2.16
P_2O_5	0.022	0.266	0.082	0.918	0.100	0.224	0.091	0.87	0.863	0.707	0.544	0.603	1.219
Total	98.00	96.40	96.72	93.78	94.131	94.371	97.12	97.74	97.21	102.1	99.21	98.00	98.32
Cr	17	<10	<10	<10	38	123	123	45	58	403	389	620	90
Ni	12	<10	10	13	22	92	72	44	19	144	143	85	40
Co	<10	<10	<10	<10	18	31	61	22	13	35	46	23	27
V	99	52	59	72	188	206	311	128	184	193	306	360	242
Zr	44	462	812	451	90	165	126	356	338	164	249	475	510
Nb	20	336	359	25	<10	27	<10	92	163	86	145	119	249
Sc	<10	<10	<10	<10	25	28	47	11	37	23	20	57	28
Y	<10	29	12	20	23	23	27	24	28	15	27	32	41
Sr	1303	1632	1243	1756	404	441	211	1894	2000	763	690	676	1323
Ba	919	3583	2123	2029	332	1277	313	3618	998	1207	1716	686	541
Rb	73	80	72	85	39	87	<10	106	73	70	177	67	46
La	11.3	–	–	–	11.6	42.3	7	–	63.4	79.6	–	101	–
Ce	21	–	–	–	27	76.6	13.5	–	141	145	–	201	–
Pr	2.18	–	–	–	3.22	7.8	2.08	–	17.7	15.3	–	24.3	–
Nd	8	–	–	–	13.8	26.8	10.1	–	67.3	53.2	–	88.3	–
Sm	1.44	–	–	–	3.24	4.64	3.07	–	11.5	7.56	–	15.4	–
Eu	0.08	–	–	–	0.82	1.2	1.09	–	2.63	2.09	–	4.55	–
Gd	0.89	–	–	–	3.55	3.95	3.63	–	7.64	5.06	–	11.1	–
Tb	0.12	–	–	–	0.48	0.6	0.66	–	1.09	0.61	–	1.42	–
Dy	0.73	–	–	–	3.05	3.54	4.52	–	6.2	3.4	–	7.66	–
Ho	0.14	–	–	–	0.66	0.73	0.92	–	1.16	0.7	–	1.29	–
Er	0.35	–	–	–	1.95	1.82	2.97	–	2.9	1.75	–	3.23	–
Tm	0.06	–	–	–	0.29	0.24	0.39	–	0.43	0.23	–	0.39	–
Yb	0.41	–	–	–	1.99	1.55	2.81	–	2.51	1.44	–	2.32	–
Lu	0.06	–	–	–	0.34	0.24	0.46	–	0.34	0.21	–	0.31	–
REE	46.76	–	–	–	71.99	172.01	53.2	–	325.8	319.91	–	462.27	–

Table 1. (Contd.)

Component	Plagiolcase–biotite rock with calcite				Biotite–calcite rock with plagioclase			Biotite carbonatite					
	Sample no.												
	313a	312	343	557	552B	420a	3411-32-2	420	563	562	561	565	568
SiO_2	36.58	41.94	39.59	36.94	28.65	20.40	30.45	11.08	14.57	11.9	11.35	10.21	8.67
TiO_2	4.53	4.42	3.16	4.46	1.64	0.98	1.23	1.09	2.57	1.28	1.27	0.99	0.97
Al_2O_3	9.45	8.42	12.42	8.68	7.96	5.03	11.24	1.86	3.55	4.10	3.92	2.96	1.95
Fe_2O_3	18.28	14.85	13.84	14.47	9.25	7.72	7.18	8.43	8.29	5.98	6.09	5.76	6.56
MnO	0.328	0.320	0.42	0.257	0.411	0.531	0.399	0.579	0.266	0.276	0.269	0.338	0.252
MgO	5.55	8.59	8.67	10.53	1.39	1.54	2.11	2.14	2.64	2.56	2.67	2.6	2.3
CaO	17.08	12.94	14.09	11.66	29.15	36.15	24.12	45.86	27.18	29.55	29.57	31.22	32.62
Na_2O	2.60	2.01	1.94	0.61	1.28	0.88	2.37	0.32	0.95	0.63	0.46	0.4	0.43
K_2O	1.44	3.46	3.53	6.33	3.77	2.45	3.79	1.65	1.27	2.11	2.16	1.83	1.01
P_2O_5	1.508	1.145	0.793	1.079	0.5	0.384	1.764	<0.003	1.401	0.692	0.636	0.821	1.511
Total	98.16	98.41	98.57	95.61	85	76.45	84.72	73.13	63.97	61.05	60.34	59.04	58.48
Cr	91	234	28	183	<10	<10	<10	<10	19	27	<10	<10	<10
Ni	85	91	74	104	10	20	18	22	16	13	15	10	13
Co	39	39	24	49	<10	<10	<10	<10	14	9	10	10	<10
V	284	284	229	250	105	48	83	106	185	99	93	127	107
Zr	492	397	392	187	79	206	1966	149	371	110	81	138	182
Nb	317	225	160	87	105	142	115	11	643	74	62	59	112
Sc	29	33	21	31	33	20	11	19	48	53	58	55	54
Y	48	30	35	24	57	67	60	69	61	64	65	72	60
Sr	1230	922	1785	698	6843	4955	2934	4887	7889	11551	11702.96	11948	11043
Ba	393	1218	1084	2054	2904	942	1962	936	1236	1791	1836	1585	1200
Rb	24	60	163	119	69	105	124	72	15	42	42	36	19
La	–	103	–	–	–	332	177	–	–	–	–	401	392
Ce	–	239	–	–	–	654	380	–	–	–	–	732	685
Pr	–	27.6	–	–	–	76.3	52.5	–	–	–	–	83.3	80.4
Nd	–	105	–	–	–	268	188	–	–	–	–	298	296
Sm	–	17.7	–	–	–	43.1	29.8	–	–	–	–	46.6	45.6
Eu	–	5.35	–	–	–	12.1	8.47	–	–	–	–	13.2	13.1
Gd	–	13.3	–	–	–	28.7	22	–	–	–	–	32.5	30.7
Tb	–	1.7	–	–	–	3.79	2.71	–	–	–	–	4	3.64
Dy	–	8.3	–	–	–	20.2	13.9	–	–	–	–	21	18.4
Ho	–	1.36	–	–	–	3.52	2.54	–	–	–	–	3.62	3.11
Er	–	3.35	–	–	–	8.89	6.32	–	–	–	–	8.78	7.43
Tm	–	0.38	–	–	–	1.15	0.8	–	–	–	–	1.13	0.87
Yb	–	2.36	–	–	–	6.93	5	–	–	–	–	6.56	5.22
Lu	–	0.35	–	–	–	0.98	0.7	–	–	–	–	1.01	0.79
REE	–	528.4	–	–	–	1458.68	889.04	–	–	–	–	1651.69	1581.47

Note: The concentrations of REE were determined by ICP-MS on a Plasma Quad instrument at the Institute of Geology of Ore Deposits, Petrography, Mineralogy, and Geochemistry, Russian Academy of Sciences; analysts A.V. Dubinin, S.A. Gorbacheva, V.D. Sinel'nikova, and L.S. Tsimlyanskaya. Other elements were measured by XRF on a Phillips PW 2400 instrument, analysts T.M. Marchenko and A.I. Yakushev. Dashes denote not analyzed.

Table 2. Chemical composition of rocks from the apical zone (oxides in wt %, trace elements in ppm)

Component	Plagiogneiss		Biotite and amphibole fenite				Pyroxene fenite					Miaskite	
	Sample No.												
	36	331	332	333	335	336	9	20	421	423	422	337	204
SiO_2	71.2	65.59	59.08	61.65	63.74	62.15	58.68	57.36	58.03	58.58	59.04	58.41	58.93
TiO_2	0.19	0.83	0.95	0.66	0.72	0.58	0.74	0.76	0.90	0.83	0.93	0.93	0.49
Al_2O_3	13.85	14.65	19.92	19.76	19.52	18.88	12.59	11.6	13.92	13.40	12.96	20.17	19.56
Fe_2O_3	1.99	5.61	4.71	3.15	3.46	4.24	7.74	10.22	8.74	9.92	8.63	4.06	3.61
MnO	0.021	0.065	0.203	0.108	0.143	0.201	0.241	0.371	0.259	0.377	0.343	0.175	0.134
MgO	0.96	1.70	1.04	0.51	0.59	0.77	0.82	0.82	0.88	0.51	0.82	0.88	1.33
CaO	3.51	2.36	1.34	0.90	0.94	1.06	3.45	2.99	3.75	3.05	3.63	1.52	1.61
Na_2O	4.65	2.86	4.24	4.51	4.35	3.03	4.64	5.78	5.44	3.89	4.38	4.54	6.37
K_2O	0.82	3.90	6.23	5.98	5.69	7.96	5.12	3.93	4.70	5.80	4.51	6.14	5.86
P_2O_5	0.050	0.350	0.281	0.093	0.090	0.205	0.353	0.435	0.404	0.299	0.273	0.139	0.061
Total	97.31	97.95	98.02	97.35	99.29	99.12	94.514	94.326	97.02	96.70	95.56	97.00	98.045
Cr	<10	<10	<10	<10	<10	<10	10	27	21	28	<10	14	<10
Ni	<10	12	13	<10	10	11	13	13	19	12	13	12	10
Co	<10	12	<10	<10	<10	<10	<10	<10	12	11	<10	<10	<10
V	20	30	39	25	28	38	99	191	108	258	92	51	23
Zr	497	511	558	408	426	755	433	516	358	452	621	355	922
Nb	196	33	184	127	155	163	223	134	217	440	349	206	188
Sc	<10	<10	<10	<10	<10	<10	19	22	<10	24	15	<10	<10
Y	34	55	48	22	41	61	34	21	18	14	22	44	31
Sr	298	325	339	265	240	282	479	308	625	1072	965	409	337
Ba	656	1927	486	486	512	510	1169	409	234	573	328	606	874
Rb	165	169	209	161	172	306	170	140	104	192	123	167	195
La	–	125	152.5	102	90.7	–	81.6	83.4	70	77.6	80.9	142	143
Ce	–	311	230	171	162	–	157	146	145	119	155	259	199
Pr	–	25.9	25.4	17.4	16.8	–	18.6	15.7	16.8	10.5	16.8	25.5	16.6
Nd	–	86.3	69.6	54.9	52.7	–	60.1	50	56.1	31	53.8	75.5	41.6
Sm	–	13.5	11.5	7.74	8.17	–	9.03	6.64	8.29	3.44	7.66	10.7	4.96
Eu	–	1.56	2.5	1.73	1.7	–	1.89	1.41	1.77	0.65	1.78	2.36	0.8
Gd	–	7.81	11.4	5.14	6	–	6.83	3.77	4.96	2.19	5.07	6.93	3.52
Tb	–	1.24	1.2	0.77	0.98	–	0.91	0.58	0.74	0.31	0.73	1.07	0.54
Dy	–	7.33	7.7	4.45	5.82	–	5.23	3.16	3.89	1.62	3.85	6.15	3.21
Ho	–	1.38	1.3	0.78	1.21	–	0.96	0.59	0.62	0.31	0.72	1.14	0.63
Er	–	4.07	3.7	2.37	3.68	–	2.72	1.65	1.98	0.78	2.12	3.43	2.02
Tm	–	0.53	0.6	0.32	0.56	–	0.39	0.22	0.24	0.15	0.27	0.43	0.3
Yb	–	3.66	4.1	2.1	3.61	–	2.66	1.84	1.59	1.31	2	2.93	2.06
Lu	–	0.48	0.6	0.25	0.52	–	0.41	0.31	0.29	0.23	0.38	0.4	0.27
REE	–	589.76	518.41	370.95	354.45	–	348.33	315.27	312.27	249.09	331.08	537.54	418.51

Table 2. (Contd.)

Component	Miaskite					Calcite-bearing miaskite							
	Sample no.												
	4	570	424	328	5-1	579	580	583	13	14	11	12	1
SiO_2	58.04	61.03	58.64	56.83	60.21	59.86	54.55	59.14	53.11	53.15	52.96	50.69	55.38
TiO_2	0.58	0.52	0.42	0.42	0.61	0.37	0.49	0.21	0.59	0.53	0.53	0.51	0.37
Al_2O_3	19.77	18.81	19.28	20.86	14.74	18.17	20.72	19.15	21.75	20.77	21.36	19.93	19.79
Fe_2O_3	4.73	3.52	3.44	3.62	4.04	4.19	3.99	1.90	3.74	2.88	4.11	4.55	3.32
MnO	0.187	0.169	0.179	0.155	0.222	0.219	0.206	0.169	0.155	0.180	0.253	0.328	0.195
MgO	0.56	0.41	0.21	0.48	1.22	0.23	0.34	0.16	0.58	0.27	0.51	0.56	0.41
CaO	2.05	1.61	2.88	2.81	4.51	3.12	3.49	3.84	2.70	4.50	3.53	7.21	4.42
Na_2O	5.78	5.60	4.13	5.69	6.59	6.40	5.85	5.24	6.58	7.25	6.45	5.52	6.34
K_2O	5.60	5.64	8.27	6.45	4.81	4.21	7.22	7.24	7.56	7.13	7.31	7.32	6.88
P_2O_5	0.085	0.047	0.031	0.075	0.058	0.071	0.130	0.008	0.192	0.078	0.078	0.177	0.118
Total	97.50	97.62	97.58	97.45	97.07	97.57	97.60	97.5	97.40	97.30	97.28	97.43	97.60
Cr	<10	10	<10	<10	<10	<10	<10	<10	<10	<10	<10	<10	<10
Ni	13	<10	<10	<10	<10	<10	<10	<10	<10	<10	10	10	<10
Co	<10	<10	<10	<10	<10	<10	<10	<10	<10	<10	<10	<10	<10
V	33	26	70	58	28	47	92	22	61	15	65	36	37
Zr	530	567	963	65	331	2014	167	42	60	109	220	91	927
Nb	165	182	185	91	231	485	182	76	172	151	173	90	196
Sc	<10	<10	<10	<10	<10	<10	<10	<10	<10	<10	<10	<10	<10
Y	26	21	<10	<10	26	17	11	15	10	11	13	19	12
Sr	667	187	2069	1981	1433	2279	3279	2909	2752	2634	2691	44348	2846
Ba	374	233	611	805	463	294	731	605	1081	925	563	847	657
Rb	196	212	203	175	209	109	188	196	182	167	207	197	194
La	95.1	–	87.6	58.1	69.1	–	–	–	80.3	80.5	88	192	64.5
Ce	143	–	132	84.9	110	–	–	–	121	125	143	291	105
Pr	13.3	–	12	7.78	10.2	–	–	–	10.9	11.4	13.5	26.5	10.1
Nd	34.8	–	33.4	23.5	30.5	–	–	–	32.4	33.4	39.5	76.1	29.1
Sm	4.5	–	4.08	2.85	4	–	–	–	3.88	4.36	4.67	9.08	3.17
Eu	0.98	–	0.81	0.56	0.85	–	–	–	0.63	0.84	0.86	1.93	0.79
Gd	3.17	–	1.8	1.95	2.37	–	–	–	2.37	2.53	1.48	3.45	2.15
Tb	0.5	–	0.27	0.27	0.42	–	–	–	0.29	0.4	0.31	0.63	0.27
Dy	3.06	–	1.44	1.55	2.69	–	–	–	1.41	2.19	1.62	3.63	1.75
Ho	0.62	–	0.24	0.37	0.54	–	–	–	0.29	0.43	0.3	0.68	0.35
Er	1.92	–	0.86	0.93	1.64	–	–	–	0.83	1.42	0.87	1.91	0.92
Tm	0.27	–	0.13	0.15	0.26	–	–	–	0.13	0.22	0.15	0.28	0.15
Yb	1.96	–	0.95	0.95	1.83	–	–	–	0.81	1.25	0.94	2.18	1.03
Lu	0.31	–	0.15	0.13	0.32	–	–	–	0.11	0.18	0.14	0.32	0.17
REE	303.54	–	275.73	183.99	234.72	–	–	–	255.35	264.12	295.34	609.69	219.45

Table 2. (Contd.)

Component	Calcite-bearing miaskites					Carbonatite						
	Sample no.											
	2	322	237	238	6	576	578	279-1	5-2	10	325	18-131
SiO_2	53.43	55.16	52.6	48.35	49.96	27.27	34.06	31.29	28.99	18.65	17.53	3.72
TiO_2	0.67	0.65	0.5	0.56	0.16	0.29	0.37	0.37	2.23	0.31	0.31	0.03
Al_2O_3	21.57	21.88	20.88	19.41	18.27	4.35	7.08	10.18	9.56	5.89	4.33	0.95
Fe_2O_3	2.15	2.07	3.78	2.17	2.61	5.4	4.51	3.92	14.6	7.57	7.70	1.8
MnO	0.158	0.154	0.154	0.249	0.304	1.481	0.982	0.967	0.948	1.657	1.692	2.397
MgO	0.31	0.24	0.54	0.38	0.38	0.16	0.2	0.49	5.62	0.48	0.43	0.26
CaO	4.10	3.74	3.34	7.82	8.52	35.16	28	24.17	19.14	38.56	38.55	59.32
Na_2O	6.53	5.72	6.17	5.42	5.61	0.72	1.42	2.05	0.6	1.25	0.88	0.41
K_2O	8.15	7.70	7.57	7.52	5.92	3.46	4.38	5.25	6.72	2.97	2.92	0.07
P_2O_5	0.052	0.047	0.123	0.082	0.194	0.025	0.24	0.419	0.329	0.159	0.161	<0.003
Total	97.20	97.41	96.00	92.06	92.25	80.39	82.83	79.50	88.74	78.31	75.28	69.00
Cr	<10	<10	<10	<10	<10	<10	<10	<10	13	<10	<10	<10
Ni	<10	<10	<10	12	12	<10	<10	14	14	18	19	19
Co	<10	<10	<10	<10	<10	<10	<10	<10	<10	<10	<10	<10
V	<20	<20	53	37	22	<20	30	23	109	24	<20	<20
Zr	91	87	225	178	241	210	211	231	97	192	177	90
Nb	175	168	156	221	144	708	669	171	1497	86	79	<10
Sc	<10	<10	10	<10	12	46	39	10	<10	18	11	28
Y	<10	10	10	15	19	63	51	40	53	82	81	65
Sr	2225	2168	2374	2655	4614	13700	10023	6936	3012	9131	9107	7291
Ba	803	779	846	758	620	346	383	416	755	475	451	64
Rb	197	201	230	217	175	81	102	204	723	141	141	33
La	53	53	–	–	160	–	–	328	250	500	–	–
Ce	85.8	85.8	–	–	242	–	–	521	417	916	–	–
Pr	8.51	8.51	–	–	22.6	–	–	49.1	41	78.6	–	–
Nd	23.7	23.7	–	–	58.9	–	–	142	123	230	–	–
Sm	2.79	2.79	–	–	6.51	–	–	18.2	16.2	30.3	–	–
Eu	0.79	0.79	–	–	1.68	–	–	4.82	3.85	8.52	–	–
Gd	1.93	1.93	–	–	4.34	–	–	12.8	9.19	22.8	–	–
Tb	0.27	0.27	–	–	0.58	–	–	1.7	1.47	3.28	–	–
Dy	1.53	1.53	–	–	3.52	–	–	10.1	8.82	20.1	–	–
Ho	0.33	0.33	–	–	0.73	–	–	1.97	1.71	4.21	–	–
Er	0.83	0.83	–	–	2.21	–	–	6.1	5.12	13.1	–	–
Tm	0.15	0.15	–	–	0.34	–	–	0.93	0.74	1.85	–	–
Yb	1.01	1.01	–	–	2.23	–	–	6.26	5.34	13.3	–	–
Lu	0.16	0.16	–	–	0.35	–	–	0.99	0.88	2.04	–	–
REE	180.8	180.8	–	–	505.99	–	–	1103.97	884.32	1844.1	–	–

Note: The concentrations of REE were determined by ICP-MS on a Plasma Quad instrument at the Institute of Geology of Ore Deposits, Petrography, Mineralogy, and Geochemistry, Russian Academy of Sciences; the analysts were A.V. Dubinin, S.A. Gorbacheva, V.D. Sinel'nikova, and L.S. Tsimlyanskaya. Other elements were measured by XRF on a Phillips PW 2400 instrument; the analysts were T.M. Marchenko and A.I. Yakushev. Dashes denote not analyzed.

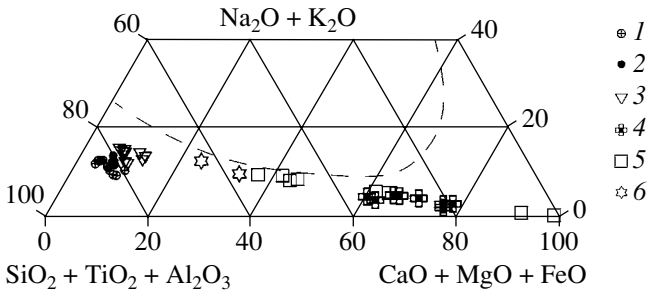

Fig. 2. Diagram of $SiO_2 + Al_2O_3 + TiO_2$–CaO + MgO + FeO–$Na_2O + K_2O$ for the (*1*) antiperthite miaskites of the Potaniny Mountains, (*2*) miaskites and (*3*) calcite-bearing miaskites of the Vishnevye Mountains, (*4*) carbonatites of the root zone, (*5*) carbonatites of the apical zone, and (6) carbonate-syenite [25].

The miaskites of the root zone differ from those of the apical part in significantly lower bulk REE contents (46.8–251 and 181–610 ppm, respectively) and a deep negative Eu anomaly (Fig. 4b).

GEOCHEMISTRY OF METASOMATIC ROCKS

The fenitization of plagiogneisses from both the root (Potaniny Mountains) and apical zones (Vishnevye Mountains) of the complex produced a decrease in SiO_2 and an increase in alkalis and Al_2O_3 from the weakly altered rear to frontal zones. The contents of MnO, Fe_2O_3, CaO, P_2O_5, and TiO_2 also increase, only decreasing in the root part at the transition to the migmatite zone. The fenites of the Potaniny Mountains show an increase in MgO content in the successive zones, whereas those of the Vishnevye Mountains show a decrease in MgO relative to the unaltered plagiogneisses. The altered amphibolites from the Potaniny Mountains show similar trends but weaker for alkalis and Al_2O_3 and more pronounced for Fe_2O_3, CaO, P_2O_5, and TiO_2 (Fig. 5).

The abundances of trace element in the metasomatic rocks after amphibolites and plagiogneisses, as well as after plagiogneisses of the root and apical zones show

Table 3. Average partition coefficients of some elements between carbonatite and nepheline syenite

Component	1	2	3	4	5	6
TiO_2	2.86	1.34	1.21	0.02	0.11	0.1–0.5
MnO	5.01	8.27	6.34	–	–	0.5–1.5
K_2O	0.39	0.59	0.58	–	–	0.4–1.5
P_2O_5	4.96	2.52	2.53	1.3	6.9	2.0–10.0
Zr	0.48	0.38	0.51	<0.012	0.23	0.1–1.5
Nb	1.81	3.43	3.04	0.09	0.67	<1
Y	5.61	2.64	3.78	0.15		<1
Sr	4.95	4.08	2.57	5.2	4.7	1.0–4.0
Ba	0.50	0.81	0.79	9.2	4.0	0.2–4.0
Rb	0.46	1.10	1.09	–	0.04	–
La	10.7	3.6	3.8	3.7	–	0.3–1.5
Ce	11.7	3.9	4.2	2.7	–	0.3–1.3
Nd	13.1	4.1	4.2	1.3	–	<1
Sm	12.7	4.2	4.6	0.6	–	0.2–1.1
Eu	308.6	5.6	5.4	–	–	0.2–1.1
Tb	12.3	4.4	5.5	0.2	–	<1

Note: (1–3) Vishnevye Gory Complex: (1) carbonatite/antiperthite miaskite of the root zone, (2) carbonatite/two-feldspar miaskite of the apical zone, (3) carbonatite/calcite-bearing miaskite of the apical zone; (4) Oldoinyo Lengai: Na carbonatite/nephelinite [26]; (5) East African rift: Ca carbonatite/phonolite [21]; (6) experimental data: carbonate melt/silicate melt [24, 27–31]. Dashes denote no data.

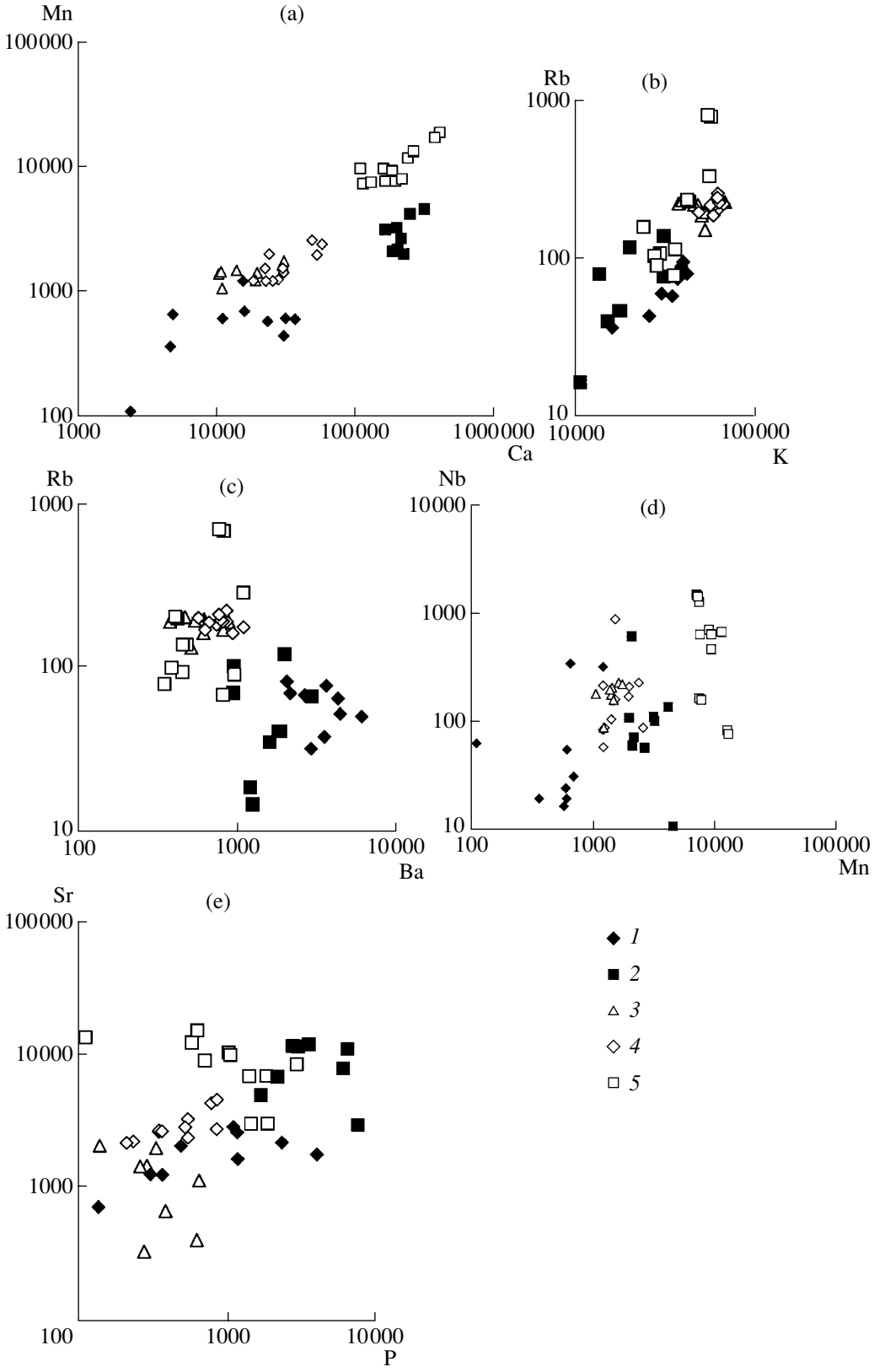

Fig. 3. Covariations of (a) Ca–Mn, (b) K–Rb, (c) Ba–Rb, (d) Mn–Nb, and (e) P–Sr in (*1, 3*, *4*) miaskites and (*2*, *5*) carbonatites of the (*1–2*) root (Potaniny Mountains) and (*3–5*) apical zones (Vishnevye Mountains).

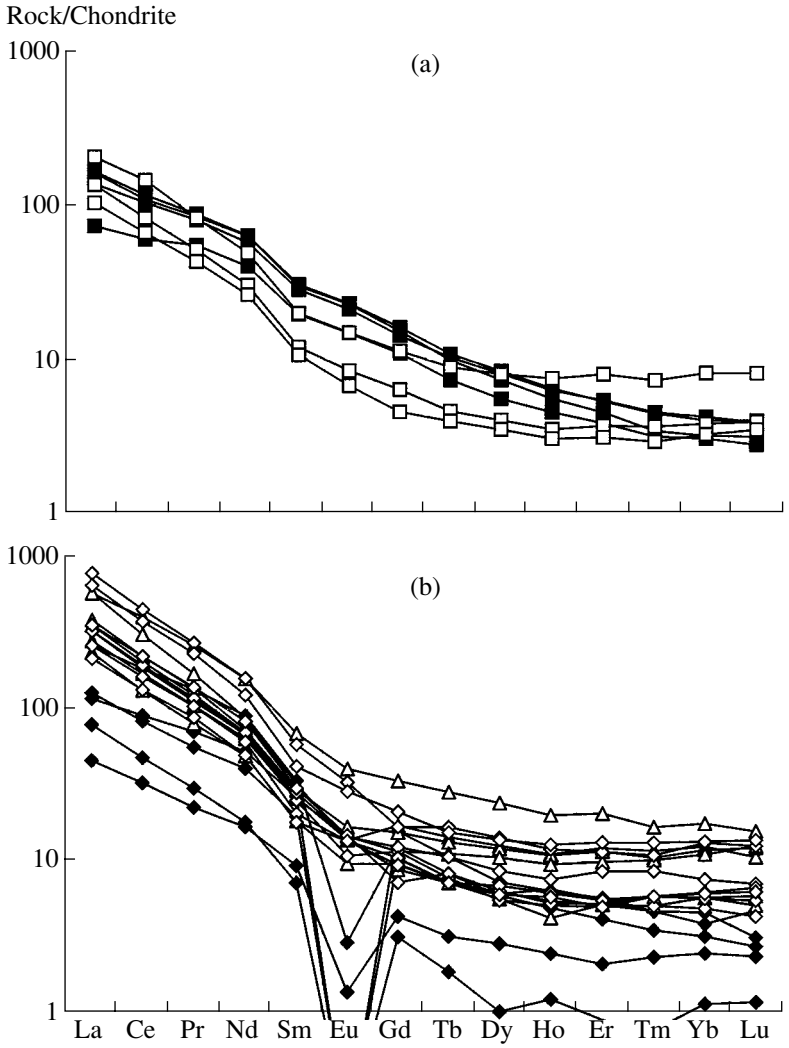

Fig. 4. Chondrite-normalized REE distribution patterns in the (a) carbonatites and (b) miaskites. Symbols are the same as in Fig. 3.

more significant differences. In particular, the high contents of Cr (up to 400 ppm), Ni (up to 144 ppm), and Co (up to 61 ppm) in the melanocratic carbonate–silicate metasomatic rocks (decreasing to the carbonatites) are indicative of their formation after amphibolites. In contrast, the contents of these elements in the fenites after plagiogneisses are close to the detection limit (Table 1).

In all cases, the Sr content and Sr/Ba, Sr/Rb, and Ba/Rb ratios increase to the frontal zones (Figs. 6a, 6b). The Ti/Nb and Mn/Nb ratios decrease in all the metasomatic associations from unaltered amphibolites or plagiogneisses to the frontal zones and carbonatites (Fig. 6c). However, these values are strongly different in the metasomatites after amphibolites and plagiogneisses. The K/Ba, K/Rb, Nb/Ta, and Zr/Hf ratios and REE distribution patterns are also indicator parameters [23].

The REE distribution patterns of the plagiogneisses show a weak negative Eu anomaly. The amphibolites have an order of magnitude lower LREE contents and an almost horizontal REE pattern. The REE contents increase in the successive metasomatic zones from amphibolites to carbonatites (Fig. 7a). The REE contents of the fenites after plagiogneisses from the root zone of the complex also increase from the rear (fenitized plagiogneisses) to frontal zones (Fig. 7b). In contrast to the preceding metasomatic zones, fenites proper, the REE distribution patterns of both migmatites and antiperthite miaskites (Fig. 4b) display a notable negative Eu anomaly. The fenites of the apical part are depleted in REE relative to the plagiogneisses (Fig. 7c).

DISCUSSION

The established geochemical features of the fenites developed after plagiogneisses in the Potaniny and Vushnevye mountains, in particular, changes in REE content relative to the miaskites, could be explained by

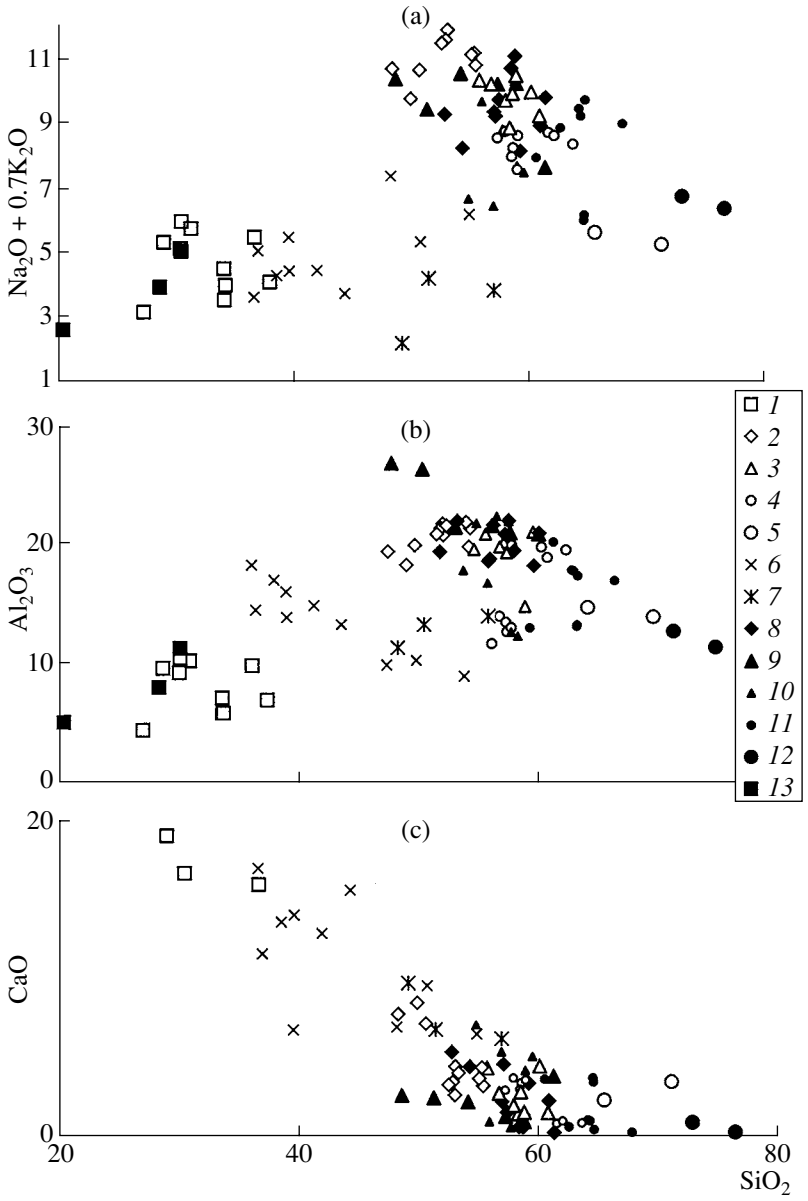

Fig. 5. Variations in the concentrations of elements in the (*1–7*) apical and (*8–13*) root zones of the complex versus SiO_2 content. (*1*, *13*) Carbonatites; (*2*) calcite-bearing miaskites; (*3*, *8*) miaskites; (*4*, *11*) fenites; (*5*, *12*) plagiogneisses; (*6*) metasomatic rocks after amphibolite (amphibole–plagioclase–biotite and calcite-bearing biotite–plagioclase rocks); (*7*) amphibolites; (*9*) migmatites; and (*10*) biotite–feldspar rocks.

the different compositions of fenitizing fluids. The fenites of the root zone could be produced by a carbonatite (fluid?), whereas those of the apical zone, by a fluid equilibrated with the miaskite.

Based on REE distribution in the successive metasomatic zones formed after the plagiogneisses of the root zone, the metasomatic process proper can be separated from the migmatization and generation of miaskites as development of the frontal metasomatic zone of the magmatic stage. A sharp decrease in REE content from the biotite–feldspar rocks to the migmatites and the deep negative Eu anomaly in the REE distribution patterns of the migmatites and antiperthite miaskites cannot be assigned to a fluid–rock interaction or fractional crystallization [32]. The Y/Ho ratios in the migmatites, antiperthite miaskites, and carbonatites of the root zone, as well as the miaskites, calcite-bearing miaskites, and carbonatites of the apical zone (Fig. 8) are usually beyond the typical magmatic range of 24–34 [32]. Only the REE distribution patterns of calcite-bearing miaskites from the apical zone are consistent with fractional crystallization.

The appearance and evolution of the Eu anomaly in the REE patterns of the antiperthite miaskites are simi-

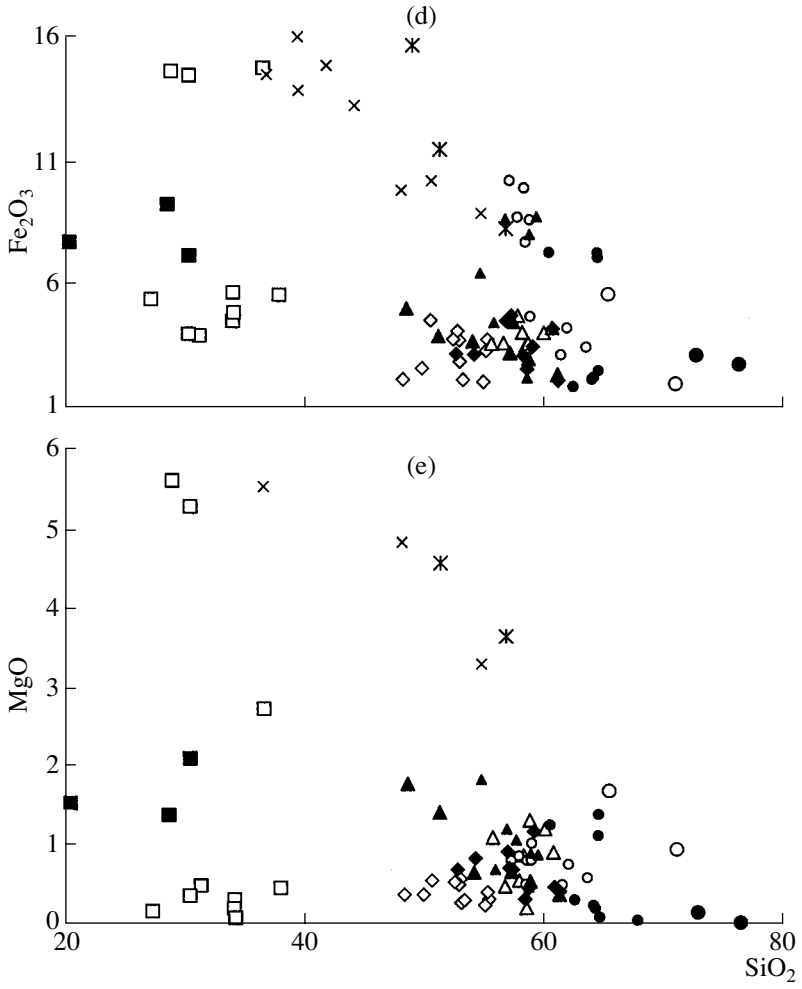

Fig. 5. (Contd.)

lar to the relationships reported by Abramov and Kurdyukov [33] for the enderbite–charnockite association and reproduced by the simulation of the fluid–magma interaction [34]. In particular, fluoride fluids equilibrated with a granitic melt show a sharp positive anomaly in REE distribution patterns increasing as temperature increases from 500 to 800°C. Thus, the migmatization and generation of miaskites was presumably caused by the percolation of high-temperature fluid through the rocks and generated alkaline magma, which controls trace-element fractionation.

According to experimental data [35], the sharp decrease of Sr/Rb (Fig. 5a) in the miaskites of the apical zone (averaging up to 10) compared with the miaskites of the Potaniny Mountains (40, on average) and carbonatites (from 24–580 to 4–220), could also be caused by the release of fluids (fluoride liquid, in the experiment) from the magma, because Rb is accumulated in the aluminosilicate melt, and Sr is accumulated in fluoride liquid.

Some trace element ratios affected by fluid-assisted fractionation (Sr/Rb, Y/Ho, LREE/HREE, Eu*, and others) in the miaskites and carbonatites [36, 37] are consistent with the concept of a palingenic–metasomatic origin of the alkaline rocks of the Vishnevye Gory Complex [18, 20, 23, 38, 39] and, together with other evidence, are at odds with their derivation [40, 41] through the crystallization of a deep-seated alkaline magma. The formation of nepheline syenites (miaskites) in linear fenite–carbonatite complexes, which complete fenitization, and their enrichment in trace elements are related to mantle carbonatite fluid flows. The mineralogical and geochemical features of these rocks, differing from those of the agpaitic nepheline syenites of ring complexes, resulted from the deep reworking of crustal material by such flows. The close association with fenites [18, 20] preceding migmatization, low Mg numbers of magmatic miaskites, agpaitic coefficients of <1, the presence of biotite instead of phlogopite and zircon instead of baddeleyite in response to the high redox potential, and SiO_2 activity in the mineral-forming environment [42] cannot be explained by the formation of miaskite magmas in the mantle.

A deep carbonatitic melt with dissolved alkaline fluid was emplaced into the plagiogneisses and

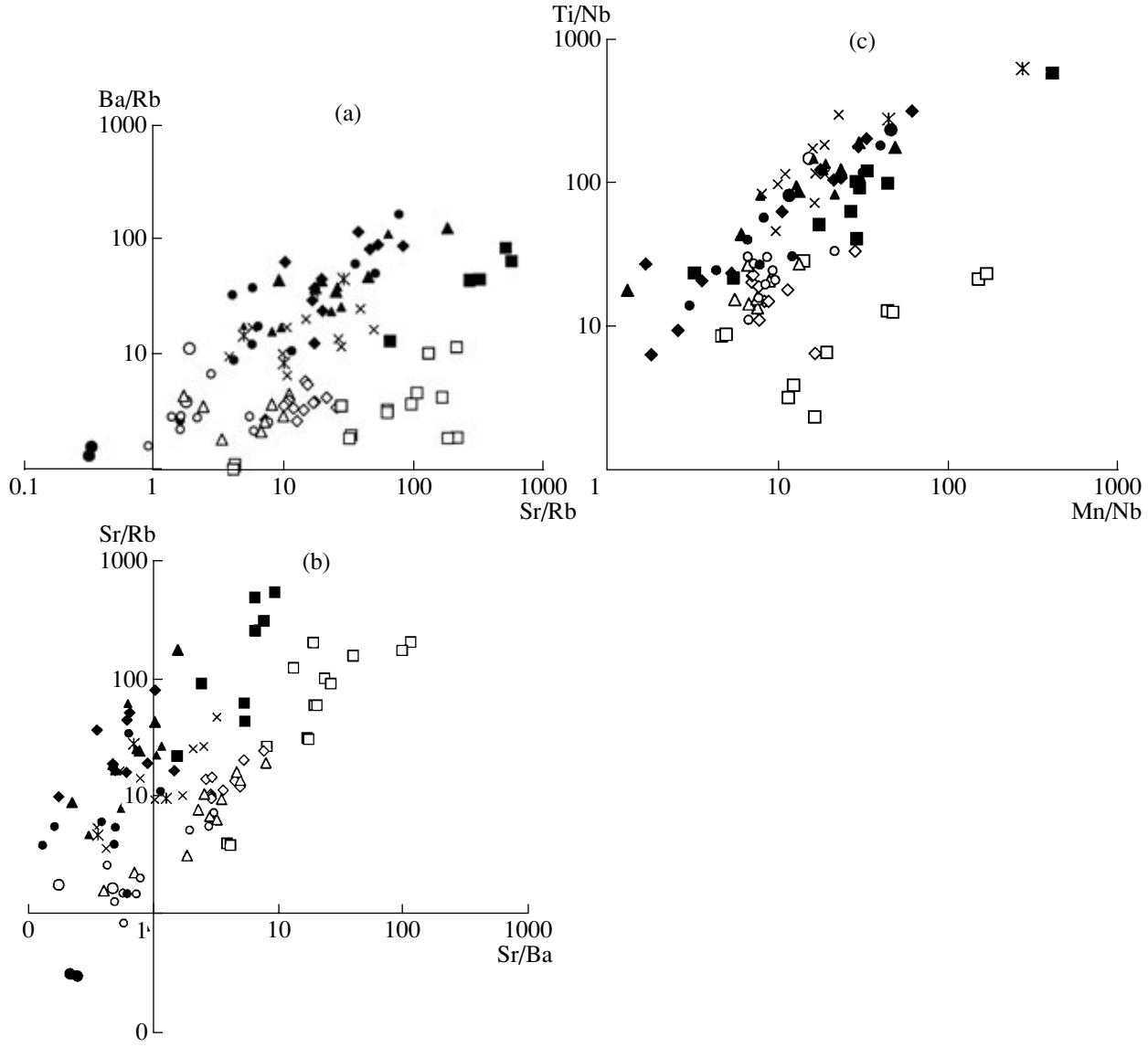

Fig. 6. Covariations of the Sr/Rb, Sr/Ba, Ba/Rb, Mn/Nb, and Ti/Nb ratios in the rocks of the complex. Symbols are the same as in Fig. 5.

amphibolites of the Vishnevye Gory Formation either directly from the mantle or from a transitional magmatic chamber. At a depth of 10–15 km and temperatures >530°C, the country rocks experienced metasomatic reworking (fenitization) under increasing temperature up to the formation of migmatites and miaskite melts at 750°C (?). The generated miaskite melt and carbonatites (with mantle isotopic signatures) ascended by 10 km into the apical zone, where fluids were equilibrated with alkaline magma and caused fenitization of the same plagiogneisses. The pressure in the apical zone is 3 kbar lower than that in the root zone, which resulted in differences in the density and composition of fluid released from the crystallizing carbonatite and silicate magmas.

The fluid regime in the root part of the complex was controlled mainly by the characteristics of the initial deep fluids and variations in the chemical composition of fluid and lower crustal rocks; whereas fluids in equilibrium with alkaline magmas were responsible for processes of the apical zone.

The possibility of such a mechanism is supported by the high water solubility (up to 10 wt % at 900°C and 0.25–2.25 kb) in carbonatite magma with the partitioning of alkalis into the fluid phase [43], high F, Cl, and alkali concentrations in the fluid phase in equilibrium with carbonatite magma [44], and efficient trace element fractionation in such fluids owing to different complexing ability in various hydrous salt liquids (carbonate, chloride, fluoride, phosphate, etc.), which are immiscible with aluminosilicate melt. In particular, the

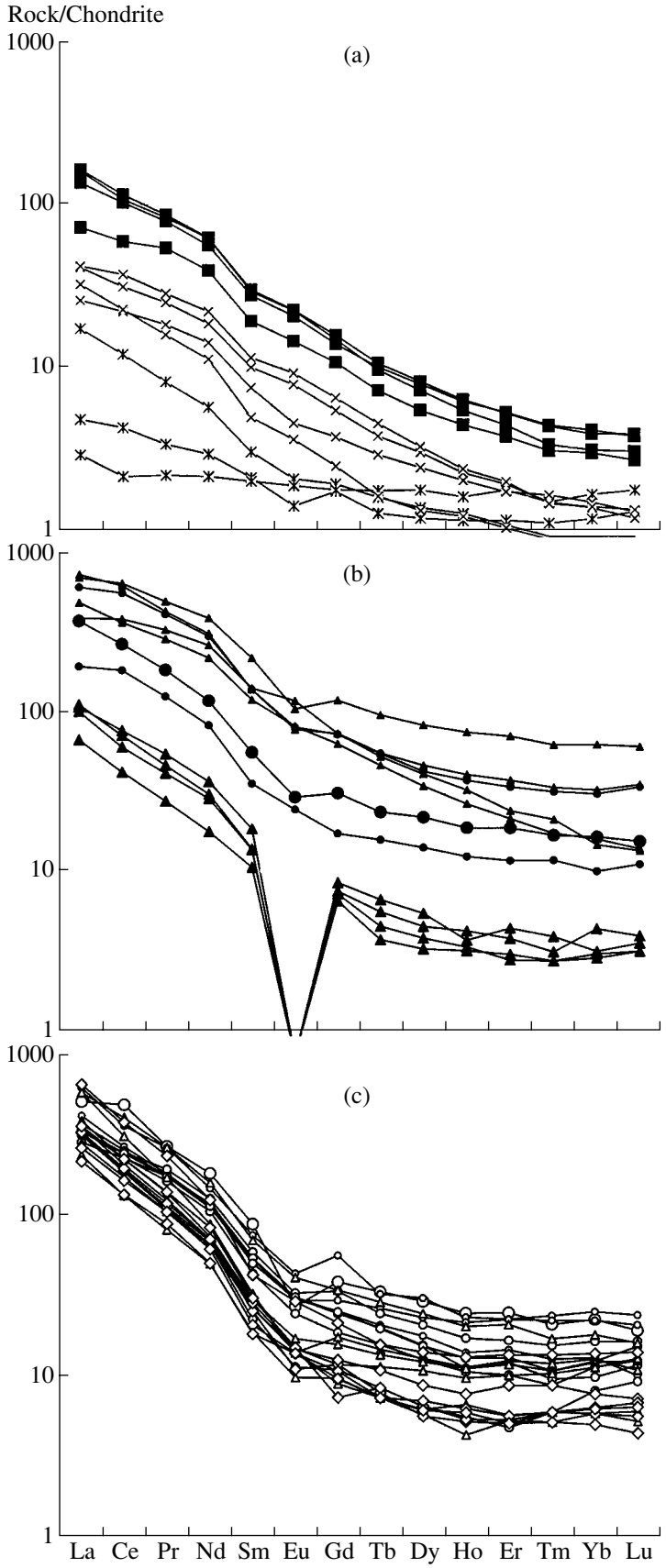

Fig. 7. Chondrite-normalized REE distribution patterns in the metasomatic rocks of the (a, b) root and (c) apical zones of the complex. Symbols are the same as in Fig. 5.

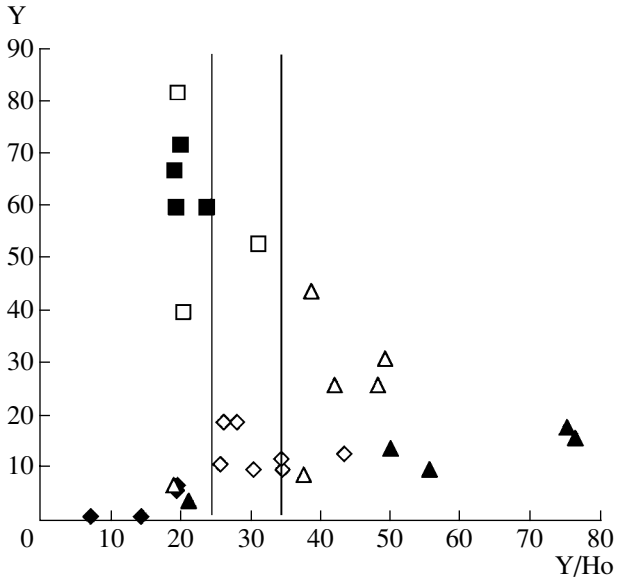

Fig. 8. Diagram of Y/Ho versus Y for the migmatites, miaskites, and carbonatites of the complex. Symbols are the same as in Figs. 3 and 5.

presence of Cl^- and F^- enhances REE partitioning into the gas phase, and the Eu partition coefficient between the fluid and the melt (at 4 kb and 800°C) is significantly higher than those of other elements [45]. The vapor phase (CO_2) is enriched in REE, especially LREE, relative to both silicate and carbonate melts at 5 kb [46].

More than 99% of the bulk REE content in natural alkaline waters occur as $LnHCO_3^{2-}$, $LnCo_3^+$, and $Ln(CO_3)_2^-$ complexes [47]. It was established that Eu^{2+} is the predominant Eu species in fluids at temperatures of more than 250°C [48], and its solubility is higher than that of trivalent REEs. The positive Eu anomaly increases with temperature in natural waters [49].

The emplacement depth of the Vishnevye Gory carbonatite massif is estimated as 10–15 km [38]. There are no known shallower carbonatites of linear zones, whereas the carbonatites of ring complexes are formed at depths of less than 5 km.

The distribution of trace elements in the Vishnevye Gory complex is not consistent with the fractional crystallization or liquid immiscibility mechanism. The occurrence of similar compositional features in the carbonatites and alkaline rocks of ring complexes can be considered indicative of element fractionation by fluids released from a carbonatite melt [37]. The scarcity of rocks with such geochemical characteristics can be related to the lower density of aqueous fluid released at shallower depths under the subvolcanic conditions of the formation of carbonatites of ring complexes.

ACKNOWLEDGMENTS

This study was supported by the Russian Foundation for Basic Research (project nos. 04-05-64817 and 06-05-64192).

REFERENCES

1. A. A. Arzamastsev, F. Bea, L. V. Arzamastseva, and P. Montero, "Rare Earth Elements in Rocks and Minerals from Alkaline Plutons of the Kola Peninsula, NW Russia, as Indicators of Alkaline Magma Evolution," Russian J. Earth Sci. **4** (3), 187–209 (2002).
2. I. Hornig-Kjarsgaard, "Rare Earth Elements in Sóvitic Carbonatites and Their Mineral Phases," J. Petrol. **39**, 2105–2121 (1998).
3. T. F. D. Nielsen and I. V. Veksler, "Is Natrocarbonatite a Cognate Fluid Condensate?," Contrib. Mineral. Petrol. **142**, 425–435 (2002).
4. V. I. Gerasimovskii, Yu. A. Balashov, and V. A. Karpushina, "Geochemistry of Rare Earth Elements in the Volcanic Rocks of the East African Rift Zones," Geokhimiya, No. 5, 515–530 (1972).
5. C. H. Donaldson, J. B. Dawson, R. Kanaris-Sotiriou, et al., "The Silicate Lavas of Oldoinyo–Lengai, Tanzania," Neues Jahrb. Mineral. Abh. **156**, 247–279 (1987).
6. D. R. Nelson, A. R. Chivas, B. V. Chappell, and M. T. McCulloch, "Geochemical and Isotopic Systematic in Carbonatites and Implications for the Evolution of Ocean-Island Sources," Geochim. Cosmochim. Acta **52**, 1–17 (1988).
7. L. N. Kogarko, P. Suddaby, and P. Watkins, "Geochemical Evolution of Carbonatite Melts in Polar Siberia," Geokhimiya, No. 2, 143–148 (1997) [Geochem. Int. **35**, 113–118 (1997)].
8. M. J. K. Flohr and M. Ross, "Alkaline Igneous Rocks of Magnet Cove, Arkansas: Mineralogy and Geochemistry of Syenites," Lithos **26**, 67–98 (1990).
9. C. Alibert, A. Michard, and F. Albarede, "The Transition from Alkali Basalts to Kimberlites: Isotope and Trace Element Evidence from Melilitites," Contrib. Mineral. Petrol. **82**, 176–186 (1983).
10. A. H. Treiman and E. J. Essene, "The Oka Carbonatite Complex, Quebec: Geology and Evidence for Silicate–Carbonate Liquid Immiscibility," Am. Mineral. **70**, 1101–1113 (1985).
11. V. A. Zharikov, N. S. Gorbachev, W. Doherty, et al., "Fractionation of Rare Earth Elements and Yttrium in Fluid–Magma Systems at High Pressures: Experimental Data," Dokl. Akad. Nauk **331**, 91–94 (1993).
12. V. Morogan, "Ijolite Versus Carbonatites as Sources of Fenitization," Terra Nova **6**, 166–176 (1994).
13. D. C. Rubbie and W. D. Gunter, "The Role of Speciation in Alkaline Igneous Fluids during Fenite Metasomatism," Contrib. Mineral. Petrol. **82**, 165–175 (1983).
14. R. F. Preston, G. Stevens, and T. S. McCarthy, "Fluid Compositions in Equilibrium with Silica-Undersaturated Magmas in the System Na_2O–Al_2O_3–SiO_2–H_2O: Clues to the Composition of Fenitizing Fluids," Contrib. Mineral. Petrol. **144**, 559–569 (2003).

15. L. M. Samson, W. Liu, and A. E. Williams-Jones, "The Nature of Orthomagmatic Hydrothermal Fluids in the Oka Carbonatites, Quebec, Canada: Evidence from Fluid Inclusions," Geochim. Cosmochim. Acta **59**, 1963–1977 (1995).
16. B. Buhn and A. H. Rankin, "Composition of Natural, Volatile-Rich Na–Ca–REE–Sr Carbonatitic Fluids Trapped in Fluid Inclusions," Geochim. Cosmochim. Acta **63**, 3781–3797 (1999).
17. A. I. Ginzburg and V. S. Samoilov, "On the Problem of Carbonatites," Zap. Vses. Mineral. O-va **112** (2), 164–176 (1983).
18. B. M. Ronenson, *Origin of Miaskites and Their Relation with Rare-Metal Mineralization* (Nedra, Moscow, 1966) [in Russian].
19. L. N. Kogarko, V. A. Kononova, M. P. Orlova, and A. R. Woolley, *Alkaline Rocks and Carbonatites of the World. Part Two: Former USSR* (Chapman– Hall, London, 1995).
20. *Alkaline–Carbonatite Complexes of the Urals* (Yekaterinburg, 1997) [in Russian].
21. V. S. Samoilov, *Geochemistry of Carbonatites* (Nauka, Moscow, 1984) [in Russian].
22. V. N. Sobachenko, A. G. Gundobin, G. P. Sandimirova, et al., "Strontium Isotopes in the Rocks of the Near-Fault Alkali Carbonate–Silicate Metasomatites and Related Carbonatites," Geol. Geofiz. **35** (3), 60–69 (1994).
23. V. S. Samoilov and B. M. Ronenson, "Geochemical Features of Alkaline Palyngenesis," Geokhimiya, No. 11, 1537–1544 (1987).
24. B. A. Kjarsgaard, "Phase Relations of a Carbonated High-CaO Nephelinite at 0.2 and 0.5 GPa," J. Petrol. **39**, 2061–2075 (1998).
25. A. V. Lapin and A. G. Zhabin, "New Type of Alkaline Carbonate–Silicate Igneous Rocks and their Petrological Significance," Dokl. Akad. Nauk SSSR **186**, 1397–1400 (1969).
26. J. Keller and B. Spettel, "The Trace Element Composition and Petrogenesis of Natrocarbonatites," in *Carbonatite Voclanism. Oldoinyo Lengai and Petrogenesis of Natrocarbonatites*, Ed. by K. Bell and J. Keller (Springer, Berlin–Heidelberg–New York, 1995), pp. 70–86.
27. B. A. Kjarsgaard, D. L. Hamilton, and T. D. Peterson, "Peralkaline Nephelinite/Carbonatite Liquid Immiscibility: Comparison of Phase Compositions in Experimental and Natural Lavas from Oldoinyo Lengai," in *Carbonatite Volcanism. Oldoinyo Lengai and Petrogenesis of Natrocarbonatites*, Ed. by K. Bell and J. Keller (Springer, Berlin–Heidelberg–New York, 1995), pp. 163–190.
28. I. C. Freestone and D. L. Hamilton, "The Role of Liquid Immiscibility in the Genesis of Carbonatites: An Experimental Study," Contrib. Mineral. Petrol. **73**, 105–117 (1980).
29. D. L. Hamilton, P. Bedson, and J. Esson, "The Behavior of Trace Elements in the Evolution of Carbonatites," in *Carbonatites. Genesis and Evolution*, Ed. by K. Bell (Unwin Hyman, London, 1989), pp. 405–427.
30. I. V. Veksler, C. Petibon, G. A. Jenner, et al., "Trace Element Partitioning in Immiscible Silicate–Carbonate Liquid Systems: An Initial Experimental Study Using a Centrifuge Autoclave," J. Petrol. **39**, 2095–2104 (1998).
31. J. H. Jones, D. Walker, D. A. Pickett, et al., "Experimental Investigations of the Partitioning of Nb, Mo, Ba, Ce, Pb, Ra, Pa and U between Immiscible Carbonate and Silicate Liquids," Geochim. Cosmochim. Acta **59**, 1307–1320 (1995).
32. M. Bau, "Controls on the Fractionation of Isovalent Trace Elements in Magmatic and Aqueous Systems: Evidence from Y/Ho, Zr/Hf, and Lanthanide Tetrad Effect," Contrib. Mineral. Petrol. **123**, 323–333 (1996).
33. S. S. Abramov and E. B. Kurdyukov, "The Origin of Charnockite–Enderbite Complexes by Magmatic Replacement: Geochemical Evidence," Geokhimiya, No. 3, 260–268 (1997) [Geochem. Int. **35**, 219–226 (1997)].
34. S. S. Abramov, "Modeling of REE Fractionation in the Acid Melt–Fluoride–Chloride Fluid System," Dokl. Akad. Nauk **376**, 798–800 (2001) [Dokl. **377**, 198–200 (2001)].
35. T. I. Shchekina and E. N. Gramenitskii, "Data on the Distribution of Rb, Sr, Ca, and Cl between Aluminosilicate and Alkali Aluminofluoride Melts," Vestn. Otd. Nauk Zemle RAN, No. 1, 20 (2002).
36. I. T. Rass, S. S. Abramov, V. A. Utenkov, and V. M. Kozlovskii, "Problems of the Genesis of the Vishnevye Gory Miaskites and Carbonatites," in *Proceedings of 21th Seminar and School on the Alkaline Magmatism of the Earth. Geochemistry of Magmatic Rocks* (Apatity, 2003), pp. 130–132 [in Russian].
37. I. T. Rass and A. V. Girnis, "Missing Eu in Carbonatites and Related Magmas: Evidence for Fluid–Melt Interaction?," in *Proceedings of 4th Eurocarb Workshop, Canary Islands, Spain, 2003* (Canary Island, 2003), pp. 14–15.
38. V. Ya. Levin and B. M. Ronenson, "On the Origin of Miaskitic Nepheline Syenites," Izv. Akad. Nauk SSSR, Ser. Geol., No. 11, 19–31 (1980).
39. B. M. Ronenson, V. A. Utenkov, and V. Ya. Levin, "Some Petrological Problems of the Ilmeny Mountains," Byull. Mosk. O-va Ispyt. Prir., Otd. Geol. **59** (1), 56–67 (1984).
40. V. A. Kononova, U. Kramm, and B. Grauert, "Age and Source of Miaskites from the Ilmeny–Vishnevye Gory Complex, Urals: Rb–Sr Isochron Data," Dokl. Akad. Nauk SSSR **273**, 1226–1230 (1983).
41. I. V. Chernyshev, V. A. Kononova, U. Kramm, and B. Grauert, "Isotope Geochronology of the Alkaline Rocks of the Urals: U–Pb Zircon Data," Geokhimiya, No. 3, 323–338 (1987).
42. I. T. Rass, S. S. Abramov, V. L. Rusinov, et al., "Conditions of the Generation and Development of Carbonatites of Linear Zones and Ring Complexes," in *Traditional and New Directions in Mineralogical Investigations* (IGEM RAN and VIMS MPR RF, Moscow, 2001), pp. 126–127 [in Russian].
43. H. Keppler, "Water Solubility in Carbonatite Melts," Am. Mineral. **88**, 1822–1824 (2003).
44. J. Gittins, M. F. Beckett, and B. C. Jago, "Composition of the Fluid Phase Accompanying Carbonatite Magma:

A Critical Examination," Am. Mineral. **75**, 1106–1109 (1990).

45. R. T. Flynn and C. W. Burnham, "An Experimental Determination of Rare Earth Partition Coefficients between a Chloride Containing Vapor Phase and Silicate Melts," Geochim. Cosmochim. Acta **42**, 685–701 (1978).
46. R. F. Wendlandt and W. J. Harrison, "Rare Earth Partitioning between Immiscible Carbonate and Silicate Liquids and CO_2 Vapor: Results and Implications for the Formation of Light Rare Earth-Enriched Rocks," Contrib. Mineral. Petrol. **69**, 409–419 (1979).
47. K. H. Johannesson, K. L. Stetzenbach, V. F. Hodge, and W. B. Lyons, "Rare Earth Element Complexation Behavior in Circumneutral pH Ground Waters: Assessing the Role of Carbonate and Phosphate Ions," Earth Planet. Sci. Lett. **139**, 305–319 (1996).
48. D. A. Sverjenskii, "Europium Redox Equilibria in Aqueous Solutions," Earth Planet. Sci. Lett. **67**, 70–78 (1984).
49. A. Michard, "Rare Earth Element Systematics in Hydrothermal Fluids," Geochim. Cosmochim. Acta **53**, 745–750 (1989).